



On the Mechanical Stability of Nickel-Based Lithium-Ion Battery Cathodes for Electric Vehicles

Muhammad Hilmy Alfaruqi

Department of Materials Science and Engineering, Chonnam National University, Gwangju 61186, Republic of Korea

Correspondence: muhammad86@chonnam.ac.kr

SUBMITTED: 9 April 2026; REVISED: 14 June 2026; ACCEPTED: 16 June 2026

ABSTRACT: $\text{LiNi}_{1-x-y}\text{Co}_x\text{Mn}_y\text{O}_2$ (NCM) cathodes are key materials for high-energy lithium-ion batteries (LIBs) for electric vehicles. However, their practical performance is limited by chemo-mechanical degradation, including anisotropic lattice strain, grain boundary stress, particle cracking, interfacial deterioration, impedance growth, and capacity fading. In this review, we provide a focused critical overview of mechanical degradation phenomena in high-energy cathode materials, with emphasis on their underlying origins, multiscale manifestations, and current mitigation strategies relevant to practical LIBs. This review aims to offer an accessible overview for both specialists and researchers newly entering the field.

KEYWORDS: Lithium-ion battery; layered oxide cathode; mechanical stability; chemo-mechanical degradation

1. Introduction

Since their commercialization by Sony in the 1990s, rechargeable lithium-ion batteries (LIBs) have been widely adopted in portable electronics and electric vehicles (EVs) [1, 2]. Their success was enabled by several notable advances, including Whittingham's pioneering demonstration of a rechargeable lithium battery using a TiS_2 cathode in 1976 [3, 4], Goodenough's development of LiCoO_2 in 1980 [5], and Yoshino's 1980s patent on a rocking-chair battery employing LiCoO_2 and petroleum coke, inspired in part by Yazami's work on lithium intercalation into graphite [6]. Figure 1 illustrates a schematic of a LIB consisting of a graphite anode and a layered cathode, between which Li ions shuttle during charge and discharge. For EV applications, cathode materials play a central role in determining the capacity and energy density of LIBs, which directly influence driving range. However, beyond range, battery lifetime is equally critical for commercialization. Most EV manufacturers define end-of-warranty performance at around 70% of the initial capacity [7]. For example, the Tesla Model S can deliver up to 659 km on a single charge and is typically backed by a battery warranty of approximately 240,000 km, corresponding to about 366 full charge/discharge cycles [8]. Similarly, the Hyundai Ioniq 5 offers a driving range of up to 569 km per charge, with a battery warranty of about 160,000 km, equivalent to roughly 282 cycles [9]. However, it is worth noting that in practical electric-vehicle operation, battery lifetime cannot be accurately inferred from warranty mileage or nominal driving range alone [10]. Although these

values may offer a general and intuitive reference for readers, they should not be interpreted as a direct measure of charge-discharge cycle life. In reality, battery degradation in electric vehicles is governed by multiple interacting factors that extend well beyond cumulative travel distance. The rate and mode of degradation depend strongly on depth of discharge, operating temperature, charge/discharge rate, charging protocol, high-voltage exposure, calendar aging, and the control strategy implemented by the battery-management system. Variations in these parameters can significantly alter the relative contributions of electrochemical, thermal, and mechanical degradation processes, even for batteries operating over similar mileage ranges. Therefore, practical battery lifetime should be understood as the outcome of coupled aging phenomena under application-specific conditions, rather than as a simple function of warranty distance or nominal cycle count.

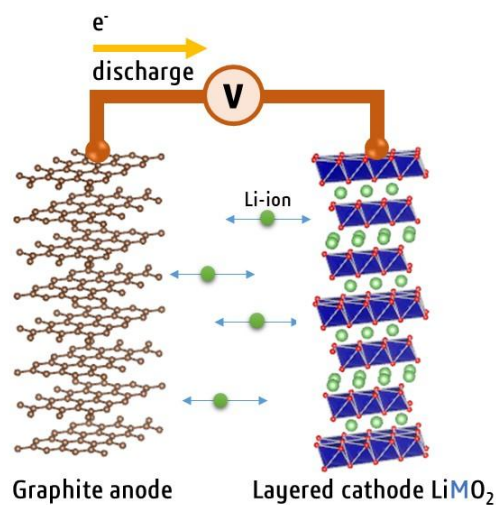


Figure 1. Schematic configuration of a lithium-ion battery.

To date, the global EV battery cathode market is split between two dominant chemistries. While Ni-rich cathodes, particularly layered nickel-containing oxides such as $\text{LiNi}_{1-x-y}\text{Co}_x\text{Mn}_y\text{O}_2$ (NCM) with various Ni/Co/Mn ratios (e.g., NCM111, NCM532, and NCM811), and $\text{LiNi}_{1-x-y}\text{Co}_x\text{Al}_y\text{O}_2$ (NCA), account for 38% of global cathode installations, LiFePO_4 has surged to 62% market share, primarily driven by China's massive deployment of cost-competitive entry-level EVs. However, in non-China markets, Ni-rich cathodes maintain dominance with ~78% market share [11]. These Ni-rich cathode materials are still favored because they offer high specific capacity and high energy density, making them attractive for long-range EV applications [12]. Nevertheless, repeated cycling inevitably induces mechanical degradation in the cathode, which progressively undermines the overall performance, durability, and safety of the battery. Numerous studies have focused on understanding and mitigating the mechanical instability of Ni-based cathodes to enhance their performance [13]. Here, we present an overview of the development of Ni-based cathodes, with particular emphasis on their mechanical stability.

It is also worth mentioning that the motivation for preparing this article arises from the growing global interest in this field, as an increasing number of researchers and industries are entering battery-related research and development. At the same time, many countries are actively pursuing advanced battery technologies as part of broader efforts toward energy transition, electrification, and strategic technological competitiveness [14]. This momentum

has been further accelerated by the expiration of a number of early foundational patents related to Li-based battery technologies [15, 16], which has lowered barriers to commercialization and enabled broader industrial participation without the same level of licensing constraints as before. In this context, the author believes that a focused critical overview highlighting the key mechanical issues of Ni-based cathodes is both timely and necessary. It is hoped that this article will serve not only the battery community but also researchers from other disciplines, particularly those who are newly entering R&D on Ni-based cathodes, by providing a swift entry point into the mechanical challenges that are highly relevant to the scope of this journal.

2. General Overview of Nickel-based Cathodes

Ni-based layered cathodes share the same fundamental crystal structure as LiCoO_2 , the cathode material originally developed by Goodenough [5]. In principle, Ni-based cathodes can be derived by replacing Co with Ni. However, in the initial development, when Co is fully substituted to form LiNiO_2 , the material suffers from rapid degradation over only a few charge/discharge cycles, rendering it unsuitable for large-scale practical applications. To address this limitation, several compositional modification strategies have been developed. Partial substitution of Ni with Co, Mn, and Al has proven particularly effective in improving structural stability, leading to widely studied compositions such as NCM and NCA [17, 18].

Each transition-metal component plays a distinct role in NCM/NCA structure [19, 20]. Ni is the primary redox-active species and contributes most of the capacity, whereas Co generally improves electronic conductivity and structural stability. Mn and Al are mainly introduced to enhance structural and thermal stability, respectively. As a result, the electrochemical performance of Ni-based cathodes is highly sensitive to composition. For example, NCM111 typically exhibits lower capacity but better structural stability than Ni-rich NCM811, which offers higher capacity at the expense of reduced durability. Figure 2 illustrates the relationship between specific capacity and capacity retention in NCM materials with varying Ni concentrations, highlighting the trade-off associated with increasing Ni content [21].

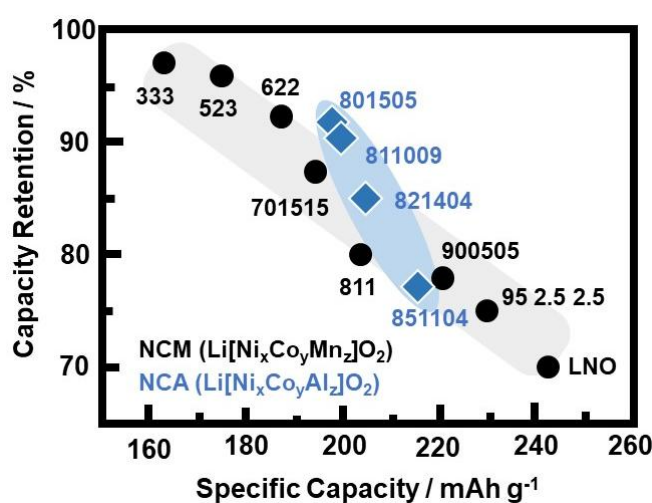


Figure 2. Trade-off between specific capacity and capacity retention in NCM cathodes with varying Ni content. All data were obtained from ref. [20].

Structurally, NCM materials adopt a layered framework composed of cubic close-packed oxygen layers, with Li and transition-metal ions occupying alternating interstitial sites (Figure 3). The transition-metal slabs are built from edge-sharing MO_6 octahedra ($\text{M} = \text{Ni}, \text{Co}, \text{Mn}$), while Li occupies the adjacent alkali layers. In Wyckoff notation, Li resides at the $3b$ sites, Ni/Co/Mn occupy the $3a$ sites, and oxygen atoms are located at the $6c$ sites. During battery operation, Li ions are extracted from the structure during charging and reinserted during discharging. It is worth noting that the theoretical capacity of NCM cathodes, which approximately 270 mAh g^{-1} , is limited by the amount of Li that can be reversibly extracted from the structure. However, the practical capacity that can be realized depends strongly on the nickel fraction and the upper voltage cut-off used during operation [22].

Upon charging, charge neutrality is maintained by increasing the oxidation states of the transition metals; for Ni, the accessible oxidation states are typically described as $\text{Ni}^{2+}/\text{Ni}^{3+}/\text{Ni}^{4+}$, while for Co they are $\text{Co}^{3+}/\text{Co}^{4+}$. Mn generally remains electrochemically inactive within the usual operating voltage range. Changes in the oxidation states of transition metals in NCM cathode have been identified through combined first-principles calculations and X-ray absorption near-edge structure analysis [23, 24]. These redox processes are accompanied by changes in metal–oxygen bond lengths and lattice parameters, which in turn alter the unit-cell volume during cycling. Such structural evolution is closely linked to the mechanical stability of NCM cathodes and plays a central role in their degradation behavior, as discussed in the following section.

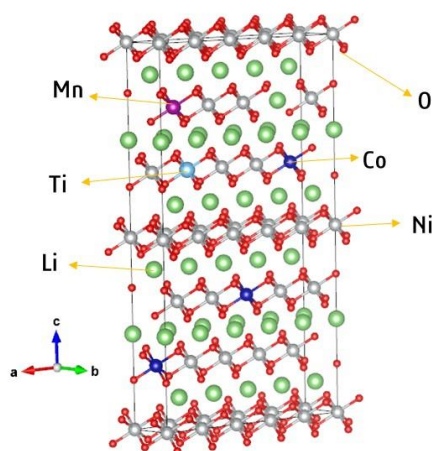


Figure 3. Illustration of NCM supercell structure with Ti doping.

3. Mechanical Stability of Nickel-based Cathodes

Mechanical stability in Ni-based NCM cathodes refers to the ability of the electrode material to maintain physical integrity and microstructural coherence during repeated lithium insertion and extraction. Unlike electrochemical stability, which generally emphasizes chemical reactivity and interfacial phenomena, mechanical stability concerns how internal stresses are generated, how cracks initiate and propagate, how electrical and ionic contacts are lost, and how particle- and electrode-level deformation accelerates degradation, even though these phenomena are ultimately driven by electrochemical reactions occurring in the electrode [13, 25].

Mechanical degradation in Ni-based cathodes must be understood not as the primary cause of performance decay but as a central element within a coupled chemo-mechanical degradation framework. The hierarchy of mechanisms begins at the atomic/lattice scale with electrochemical delithiation, which produces anisotropic lattice strain and abrupt phase transitions, most notably the H2 → H3 transition [26]. These lattice-level changes generate substantial internal stresses that concentrate at grain boundaries and crystallographic defects, leading to the nucleation and propagation of intergranular and intragranular microcracks. The mechanical damage that ensues is both a consequence and an accelerator of chemical degradation. Crack formation exposes fresh, highly reactive cathode surfaces to the electrolyte, promoting oxygen release, transition-metal dissolution, surface reconstruction into ionically resistive rock-salt-like phases, and growth of a thick cathode–electrolyte interphase (CEI). These chemical and interfacial changes, in turn, reduce fracture toughness, increase mechanical heterogeneity, and intensify local stress concentrations [27]. This coupled, hierarchical perspective highlights that while mechanical fracture is often the most visible manifestation of degradation and a dominant contributor to long-term fade, it is neither independent of nor hierarchically superior to the underlying electrochemical and chemical processes. Instead, the three domains are inextricably linked in a self-reinforcing cycle.

In Ni-rich NCM cathodes, mechanical degradation becomes especially severe because the pursuit of higher energy density typically requires deep delithiation and elevated upper cutoff voltages. Under these conditions, the lattice undergoes more pronounced anisotropic changes, which intensify internal stress accumulation during cycling. Differential capacity (dQ/dV) analysis indicated multiple peaks during charge-discharge, evidencing sequential phase transitions in NCM [28]. This effect becomes markedly stronger at very high Ni contents; for example, materials with Ni \approx 0.95 can exhibit a c -axis variation of about 6.9%, compared with only \sim 2.6% in NCM 0.6, indicating a substantially greater structural instability in the Ni-rich regime. Under such conditions, lattice-parameter variation and strain heterogeneity become more severe, generating stress fields large enough to fracture particles, separate grains, disrupt conductive networks, and ultimately cause capacity decay and impedance rise. A primary source of mechanical instability originates from anisotropic lattice transformations during lithium (de)intercalation. Layered NCM structures undergo changes in interplanar spacing, particularly along the c -axis, as well as changes in the a lattice parameter upon lithium extraction [28].

Practical NCM particles are typically secondary particles composed of many micron- or submicron-sized primary grains, anisotropic strain cannot be accommodated smoothly across the entire particle. This intergranular strain mismatch leads to stress concentration at grain boundaries, promotes intergranular delamination, and opens microcrack pathways that can eventually propagate throughout the secondary particle. The direct consequence of such mechanical damage is the loss of electrical and ionic connectivity. Microcracks formed within secondary particles can isolate active domains from the carbon conductive network or from effective ionic pathways, rendering portions of the material electrochemically inactive even though they remain chemically capable of storing lithium. Cracking also increases the effective surface area exposed to the electrolyte, thereby accelerating parasitic reactions and promoting faster growth of the cathode–electrolyte interphase (CEI), which further increases impedance [28].

In addition, mechanical degradation in Ni-based layered cathodes evolves hierarchically across multiple length scales, from lattice distortion at the atomic level to impedance growth and capacity decay at the full-cell level. This multiscale degradation originates from strong chemo-mechanical coupling during repeated delithiation and lithiation, whereby concentration-dependent structural deformation generates internal stress, fracture, and progressive electrochemical instability. A mechanistic understanding therefore requires connecting structural changes across scales rather than treating cracking or capacity fading as isolated phenomena.

At the primary-particle scale, the anisotropic lattice response does not remain spatially uniform. Instead, lithium concentration gradients develop within individual particles during cycling, leading to heterogeneous local strain and intragranular stress accumulation. Because different regions of a particle experience different extents of expansion and contraction, tensile stress can develop locally and initiate cracks within the grain interior. These intragranular cracks are particularly detrimental because they reflect the direct conversion of lattice-scale chemo-mechanical mismatch into particle-scale fracture. At the secondary-particle level, the degradation becomes further amplified by the polycrystalline architecture of agglomerated primary grains. Adjacent grains often differ in crystallographic orientation, state of lithiation, and local mechanical response, leading to stress mismatch at grain boundaries. Repeated cycling therefore promotes grain-boundary decohesion and intergranular cracking, which can propagate radially through the secondary particle. Once formed, these cracks expose fresh internal surfaces to the electrolyte and create new pathways for electrolyte infiltration, thereby coupling internal mechanical damage with accelerated chemical degradation. The consequences of particle fracture extend to the electrode scale. Cracking and fragmentation of active materials disrupt electronic percolation pathways, weaken binder-mediated interparticle connectivity, and alter the pore structure of the composite electrode. These changes can increase tortuosity, modify porosity distribution, and contribute to electrode swelling during long-term cycling. At the same time, crack surfaces formed within and between particles promote deeper electrolyte penetration and more extensive parasitic interfacial reactions, including surface reconstruction and resistive interphase formation. Such changes progressively deteriorate both ionic and electronic transport throughout the electrode. Ultimately, these structural and interfacial degradations manifest at the cell level as impedance growth, reversible-capacity loss, reduced rate capability, and increased safety risk.

Further, it is also important to note that although mechanical degradation of Ni-based NCM cathodes is often discussed from the perspective of intrinsic material instability, its practical evolution in real cells is also strongly influenced by electrode-level architecture. For example, binder distribution and adhesion determine how effectively mechanical stress is transferred or relaxed between active particles, conductive additives, and the current collector, thereby affecting cohesion, crack propagation, and particle isolation during repeated cycling.

Electrode porosity also plays important roles. Sufficient pore volume can buffer local volume changes and facilitate electrolyte infiltration, whereas excessive densification or nonuniform pore collapse may increase local stress concentration and tortuosity, aggravating transport limitations and mechanical damage. In addition, calendaring, while beneficial for improving electrode density and interparticle contact, can simultaneously reduce strain tolerance and amplify internal stress heterogeneity, especially in Ni-rich cathodes that already undergo substantial anisotropic volume change. Therefore, the mechanical degradation of

NCM cathodes should be understood as a multiscale phenomenon in which intrinsic particle fragility interacts with electrode processing, mesoscale structural heterogeneity, and composite-electrode mechanics.

Prior work on NMC composite cathodes reported initial porosities of 0.42–0.487, minimal attainable porosities of 0.225–0.254, and final porosities of 0.213–0.270 even under the same calendaring condition (75 °C, 56 MPa), together with hardness values up to ~150 MPa [29]. These results indicate that electrode processing strongly affects stress accommodation, contact retention, and transport pathways, thereby modulating how intrinsic particle-level degradation evolves at the electrode scale.

Recent work on high-loading NMC622 and NMC811 cathodes further illustrates that electrode-level mechanical behavior strongly mediates practical degradation [30]. In that study, severe calendaring reduced the final porosity from ~36.8 - 38.2% to only ~6.1–7.2%, accompanied by substantial densification (e.g., NMC811: 2.95 to 4.67 g cm⁻³; NMC622: 3.02 to 4.47 g cm⁻³) at areal capacities of ~4 mAh cm⁻². This low-porosity state significantly increased the mechanical stiffness of the composite electrode: for NMC811, the elastic modulus and hardness increased from 3.86 ± 0.28 GPa and 0.07 ± 0.008 GPa to 32.05 ± 3.05 GPa and 0.90 ± 0.17 GPa, respectively, while for NMC622 they increased from 2.02 ± 0.28 GPa and 0.027 ± 0.002 GPa to 18.62 ± 2.06 GPa and 1.22 ± 0.06 GPa. At the same time, electrolyte uptake decreased sharply, from ~33.15% to 8.54% for NMC811 and from ~32.12% to 5.73% for NMC622, demonstrating the classical trade-off between mechanical/electronic reinforcement and ionic transport margin. Importantly, severe calendaring also induced microcracking in active-material particles, indicating that electrode processing itself can introduce mechanical damage. Nevertheless, the denser electrodes showed improved particle-to-particle contact, stronger adhesion, and better rate/cycling behavior under the studied conditions. These results suggest that the degradation of Ni-rich NCM cathodes is governed not only by intrinsic particle fragility but also by electrode porosity, densification history, and the resulting balance between contact retention, transport limitation, and stress accumulation.

Further evidence that electrode-level mechanics critically mediate degradation comes from calendaring studies on high-Ni LiNi_{0.9}Mn_{0.05}Al_{0.05}O₂ cathodes [31]. In that work, cathode porosity was reduced from ~55% in the uncalendered state to 45%, 35%, and 25%, and SEM analysis showed that high-Ni secondary particles fractured at all calendaring levels, with pronounced cracking/pulverization at 35% and 25% porosity. Calendaring also increased the effective cathode surface area by approximately 376%, which would conventionally be expected to accelerate parasitic reactions. However, full cells cycled at C/2 between 2.5 and 4.3 V for 500 cycles exhibited improved capacity retention with calendered electrodes, increasing from ~70% for uncalendered cathodes to ~75–76% for cathodes calendered to 45–25% porosity. In addition, impedance/polarization growth was slower for the more heavily calendered electrodes, and pulse-power analysis indicated a substantially broader usable capacity range after aging. These results suggest that although calendaring can introduce particle fracture and increase reactive surface area, the concurrent improvement in interparticle contact and composite-electrode mechanical cohesion can suppress contact-loss-driven degradation during long-term cycling.

Current strategies for improving mechanical stability operate simultaneously at multiple levels: crystal- and composition-level design to reduce strain, particle-architecture engineering to suppress crack initiation, surface engineering to resist damage that triggers fracture, and

electrode engineering to preserve cohesion and contact during repeated expansion and contraction. One of the most prominent approaches is the use of single-crystal NCM particles [32]. Operando X-ray computed tomography studies have shown that, compared with conventional polycrystalline counterparts, single-crystalline NMC811 exhibits markedly improved structural integrity during cycling, with substantially reduced crack formation and particle disintegration (Figure 4). By eliminating the internal grain-boundary network characteristic of polycrystalline secondary particles, single-crystal materials suppress the intergranular cracking that is typically dominant in conventional morphologies [33]. Optimization of particle-size distribution, electrode density, and electrolyte formulation remains necessary to ensure that mechanical gains are not offset by chemical penalties.

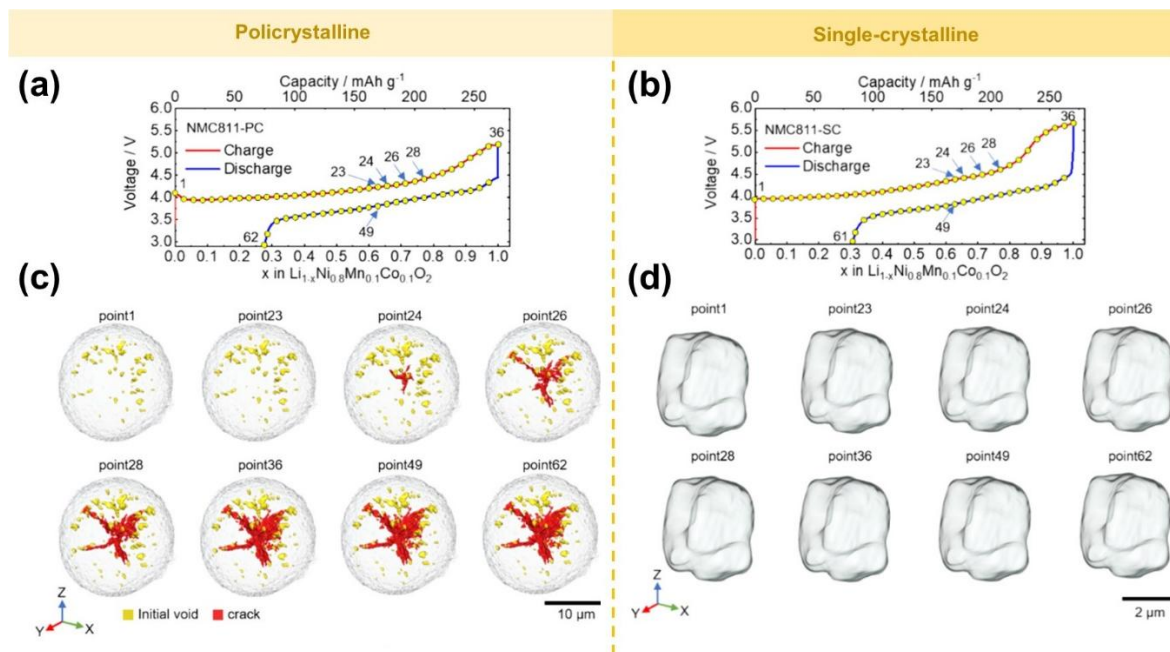


Figure 4. Operando X-ray CT results for NMC811. Voltage profiles of (a) polycrystalline and (b) single-crystalline NMC811 during charge/discharge at 0.5 C. Corresponding 3D-rendered images at selected states during cycling for (c) polycrystalline and (d) single-crystalline NMC811. Reprinted with permission from ref. [33], copyright 2024 American Chemical Society.

Another well-established structural strategy is the use of concentration-gradient or core-shell architectures (Figure 5), in which the core remains Ni-rich to preserve capacity while the near-surface region is enriched with Mn/Co or stabilized by dopants that improve resistance to phase transitions and oxygen release [34]. From a mechanical standpoint, a more stable outer region can act as a protective shell that suppresses or at least delays crack propagation while simultaneously reducing side reactions that weaken the surface. Composition gradients may also smooth the stress distribution because elastic properties and chemical expansion coefficients vary gradually rather than discontinuously. In addition to compositional grading, bulk doping with elements such as Al, Mg, Ti, Zr, Nb, W, or Mo is widely employed to stabilize the layered structure and reduce the amplitude of lattice changes at high state of charge, particularly those associated with the phase transition [35]. When lattice variation becomes smaller and more reversible, internal stress is reduced and the probability of fracture decreases. Doping may also strengthen grain boundaries or suppress cation migration that promotes

mechanically fragile surface phases, meaning that its benefits are not solely electrochemical but also mechanical.

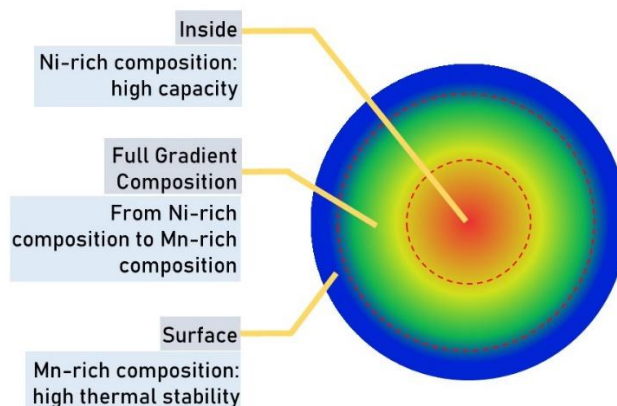


Figure 5. Schematic showing how a concentration-gradient design is applied to an NCM cathode to tailor transition metal distribution across the particle.

Conformal surface coatings, including oxides, phosphates, niobates, and fluorides, were initially developed to improve interfacial stability, but they also provide important mechanical benefits [36, 37]. An appropriately designed coating can act as a near-surface crack inhibitor, suppress surface corrosion and phase reconstruction that embrittle the outer layer, and help prevent local reactions from accelerating structural damage. However, coatings also introduce potential mechanical risks and unoptimized coating thickness may induce deterioration of cathode performance. For example, Li et al. investigated PPy coating on Ni-rich NCM cathodes and demonstrated that while an ultrathin layer of approximately 3 nm effectively buffers the anisotropic lattice strain and volume changes associated with the H2 → H3 phase transition suppresses microcrack propagation and maintains surface electronic conductivity thereby interrupting the chemo-mechanical feedback loop and enhancing long-term capacity retention excessively thick PPy layers suffer from repeated swelling and shrinking that leads to poor interfacial adhesion mechanical shedding delamination and loss of active material contact resulting in accelerated performance decay [38]. In addition, Wang et al. studied the optimization of Al₂O₃ coating thickness applied via atomic layer deposition and showed that an optimal ultrathin coating corresponding to 10 ALD cycles functions as an effective chemical barrier that passivates the surface against electrolyte attack and oxygen release while adding minimal impedance yielding superior cycling stability with 88% capacity retention after 300 cycles at 1C rate between 2.7 and 4.3 V compared with only 35.3% for the pristine material [39]. By contrast thicker Al₂O₃ layers substantially increase charge-transfer resistance and block Li-ion diffusion pathways owing to the insulating character of alumina thereby reducing initial discharge capacity from 214.08 to 178.80 mAh g⁻¹ and degrading rate capability. These findings together illustrate a characteristic volcano-shaped dependence of electrochemical performance on coating thickness and reinforce that both PPy and Al₂O₃ coatings prove beneficial only when they simultaneously satisfy the criteria of minimal strain mismatch robust interfacial bonding unimpeded Li-ion transport and high chemical stability thereby mitigating rather than exacerbating the coupled chemo-mechanical degradation loop in Ni-based cathodes.

Although comprehensive head-to-head studies directly comparing the various mitigation strategies for Ni-based cathodes remain limited, and further systematic investigation is still required, Table 1 is proposed as an initial comparative framework. Rather than providing a definitive ranking, this table offers a mechanism-informed overview of representative approaches, highlighting their respective strengths, limitations, and likely influences on strain accommodation, Li⁺ transport, chemical stability, and cycling performance. In this way, the comparison is intended to serve as a preliminary insight for identifying promising design directions to disrupt the chemo-mechanical degradation loop.

Table 1. Comparison of representative mitigation strategies for Ni-based NCM cathodes.

Strategy	Primary Mechanism	Effectiveness on Chemo-Mechanical Loop	Chemical Stability	Possible Key Limitations
Elastic polymer coating	Compliant cushioning, strain absorption, homogeneous Li distribution	High	Moderate to good	Delamination/shedding at excessive thickness
Inorganic ALD coating	Surface passivation, suppression of oxygen evolution and HF formation	High (indirect via reduced reactivity)	Excellent	Increased charge-transfer resistance, lower initial capacity
Single-crystal morphology	Elimination of grain boundaries	High	Moderate	Relatively more complex synthesis
Elemental doping	Lattice stabilization, reduced anisotropic contraction	Moderate	Moderate	Limited surface protection
Core-shell / concentration gradient	Graded strain distribution	High	Good	Synthesis complexity, interfacial stability
Hybrid coating	Combined cushioning and passivation	Very high	Excellent	Process complexity

Looking forward, future development increasingly emphasizes controlling fracture from the outset through a mechanics-by-design philosophy. This includes multiscale chemomechanical modeling to predict crack-initiation sites from lattice evolution and Li-concentration gradients, together with atomistic, phase-field, and finite-element simulations that link local structural instability to particle-scale fracture [40]. Such approaches can accelerate exploration of broad chemical and microstructural design spaces, including dopant selection, coating feasibility, and gradient-composition architectures that are difficult to optimize experimentally alone. In parallel, artificial intelligence and machine-learning tools are emerging as useful accelerants for materials discovery by identifying structure–property relationships, screening promising chemical configurations, and guiding closed-loop optimization between computation and experiment [41].

Beyond chemistry, future progress will also require grain-boundary and texture engineering to improve strain compatibility, and particle architectures that balance mechanical robustness with rapid ion transport. With those integrated strategies, NCM cathodes may move closer to industrial targets of high energy density, long cycle life, acceptable rate capability, and controlled safety risk, although operation at high state of charge will continue to impose unavoidable trade-offs among energy, lifetime, and mechanical robustness. Finally, beyond electrochemical considerations, the reliance on Co is increasingly viewed as unsustainable because of cost, resource constraints, toxicity, and persistent environmental and ethical

concerns surrounding its supply chain. Accordingly, Co-free cathodes such as $\text{LiNi}_{1-x-y}\text{Mn}_x\text{Al}_y\text{O}_2$ (NMA) have emerged as promising alternatives [18, 42].

4. Conclusions

In summary, mechanical stability has emerged as a central challenge for NCM cathodes because the pursuit of higher energy density inevitably intensifies lattice strain, intergranular stress, crack formation, and loss of electrochemical connectivity. These mechanically driven degradation processes are closely intertwined with interfacial chemical reactions, making them a major barrier to long cycle life, rate capability, and safety. Recent progress has shown that meaningful improvements can be achieved through integrated strategies, including single-crystal and gradient particle designs, bulk doping, surface protection, and electrode-level optimization. Further advances will likely depend on a more unified mechanics-by-design approach, in which crystal chemistry, particle architecture, interface engineering, and operating protocols are co-optimized rather than developed independently. In particular, future research should focus on understanding crack initiation across multiple length scales, improving strain accommodation without sacrificing transport kinetics, and establishing design rules that remain compatible with industrial manufacturing. Those efforts will be essential for enabling NCM cathodes to deliver high energy density together with the durability and robustness required for practical applications.

Acknowledgments

The author would like to dedicate this work to Professor Jaekook Kim. The author is deeply grateful for his unwavering support and guidance, which began during the author's time as a student and has continued to shape author's career. As a pioneering co-inventor of nickel-based cathode materials, having mentored under the distinguished Professor Arumugam Manthiram and the 2019 Nobel Laureate in Chemistry, the late Professor John B. Goodenough, Professor Jaekook Kim has been a constant source of inspiration. His profound scientific insights and commitment to excellence have not only guided this research but also fundamentally shaped the author's scientific perspective.

Competing Interest

The author declares that the author has no known competing financial interests or personal relationship that could have appeared to influence the work reported in this paper.

References

- [1] Armand, M.; Tarascon, J.-M. (2008). Building better batteries, *Nature*, 451, 652-657. <https://doi.org/10.1038/451652a>.
- [2] Hernandha, R.F.H. (2025). Research, development, and innovation insights for solid-state lithium battery: laboratory to pilot line production, *Discover Electrochemistry*, 2, 26. <https://doi.org/10.1007/s44373-025-00040-y>.

- [3] Whittingham, M.S. (1976). Electrical energy storage and intercalation chemistry, *Science*, 192, 1126-1127. <https://doi.org/10.1126/science.192.4244.1126>.
- [4] Whittingham, M.S.; Gamble Jr, F.R. (1975). The lithium intercalates of the transition metal dichalcogenides, *Materials Research Bulletin*, 10, 363-371. [https://doi.org/10.1016/0025-5408\(75\)90006-9](https://doi.org/10.1016/0025-5408(75)90006-9).
- [5] Mizushima, K.; Jones, P.C.; Wiseman, P.J.; Goodenough, J.B. (1980). Li_xCoO_2 ($0 < x < 1$): A new cathode material for batteries of high energy density, *Materials Research Bulletin*, 15, 783-789. [https://doi.org/10.1016/0025-5408\(80\)90012-4](https://doi.org/10.1016/0025-5408(80)90012-4).
- [6] Yazami, R.; Hamwi, A. (1988). A new graphite fluoride compound as electrode material for lithium intercalation in solid state cells, *Solid State Ionics*, 28, 1756-1761. [https://doi.org/10.1016/0167-2738\(88\)90456-0](https://doi.org/10.1016/0167-2738(88)90456-0).
- [7] Liu, Y.; Wang, X.-L. (2025). Warranties of batteries: Requirements, state-of-the-art, relevant analysis methods, and research perspectives, *Journal of Reliability Science and Engineering*, 1, 032003. <https://doi.org/10.1088/3050-2454/ae033b>.
- [8] Tesla: Vehicle Warranty. (accessed on 9 April 2026) Available online: <https://www.tesla.com/support/vehicle-warranty>.
- [9] Hyundai: Warranty Information. (accessed on 9 April 2026) Available online: <https://www.hyundai.com/kr/en/customer-service/car-management-service/warranty-period/normal-period/rv>.
- [10] Karunarathna, J.S.; Madawala, U.K.; Sandelic, M.; Blaabjerg, F.; Baguley, C. (2023). The impact of operational and environmental conditions on battery lifetime in fast electric vehicle charging systems, *IEEE Transactions on Power Electronics*, 39, 4645-4656. <https://doi.org/10.1109/TPEL.2023.3342121>.
- [11] SNE Research: From Jan to Dec 2025, Global EV Battery Cathode Installment Reached 2,649K ton, a 35.3% YoY Growth. (accessed on 9 April 2026) Available online: https://www.sneresearch.com/en/insight/release_view/593/page/0
- [12] Gao, Z.-W.; Lan, T.; Yin, H.; Liu, Y. (2025). Development and commercial application of lithium-ion batteries in electric vehicles: a review, *Processes*, 13, 756. <https://doi.org/10.3390/pr13030756>.
- [13] Huang, H.; Lyu, Y.; Dong, S.; Guo, Z.-S. (2025). Chemo-mechanical degradation in polycrystalline $\text{LiNi}_x\text{Co}_y\text{Mn}_{1-x-y}\text{O}_2$ cathodes: Intergranular fracture and electrochemical behavior, *Engineering Fracture Mechanics*, 325, 111327. <https://doi.org/10.1016/j.engfracmech.2025.111327>.
- [14] Munonye, W.C.; Ajonye, G.O.; Ahonsi, S.O.; Munonye, D.I.; Chigozie, I.O.; Akinloye, O.A. (2026). Advancing circularity in battery systems for renewable energy: Technologies, barriers, and future directions, *Advanced Energy and Sustainability Research*, 7, e202500255. <https://doi.org/10.1002/aesr.202500255>.
- [15] Thackeray, M.M.; Johnson, C.S.; Amine, K.; Kim, J. (2004). Lithium metal oxide electrodes for lithium cells and batteries, US Patent, US6680143B2.
- [16] Goodenough, J.B.; Padhi, A.K.; Nanjundaswamy, K.; Masquelier, C. (2003). Cathode materials for secondary (rechargeable) lithium batteries, US Patent, US6514640B1.
- [17] Liu, Z.; Yu, A.; Lee, J.Y. (1999). Synthesis and characterization of $\text{LiNi}_{1-x-y}\text{Co}_x\text{Mn}_y\text{O}_2$ as the cathode materials of secondary lithium batteries, *Journal of Power Sources*, 81, 416-419. [https://doi.org/10.1016/S0378-7753\(99\)00221-9](https://doi.org/10.1016/S0378-7753(99)00221-9).
- [18] Li, W.; Lee, S.; Manthiram, A. (2020). High-nickel NMA: a cobalt-free alternative to NMC and NCA cathodes for lithium-ion batteries, *Advanced Materials*, 32, 2002718. <https://doi.org/10.1002/adma.202002718>.

- [19] Hu, W.; Chen, Y.; Wang, Y.; Zhu, H.; Li, G.; Li, H. (2022). Unraveling the roles of Al, Mn and Co in the Ni-rich cathode material for Li-ion batteries, *Colloids and Surfaces A: Physicochemical and Engineering Aspects*, 648, 129185. <https://doi.org/10.1016/j.colsurfa.2022.129185>.
- [20] Jung, S.K.; Kim, H.; Song, S.H.; Lee, S.; Kim, J.; Kang, K. (2022). Unveiling the role of transition-metal ions in the thermal degradation of layered Ni–Co–Mn cathodes for lithium rechargeable batteries, *Advanced Functional Materials*, 32, 2108790. <https://doi.org/10.1002/adfm.202108790>.
- [21] Yoon, C.S.; Park, K.-J.; Kim, U.-H.; Kang, K.H.; Ryu, H.-H.; Sun, Y.-K. (2017). High-energy Ni-rich $\text{Li}[\text{Ni}_x\text{Co}_y\text{Mn}_{1-x-y}]\text{O}_2$ cathodes via compositional partitioning for next-generation electric vehicles, *Chemistry of Materials*, 29, 10436-10445. <https://doi.org/10.1021/acs.chemmater.7b04047>.
- [22] Gao, D.; Huang, Y.; Dong, H.; Li, C.; Chang, C. (2023). Atomic horizons interpretation on enhancing electrochemical performance of Ni-Rich NCM Cathode via W doping: dual improvements in electronic and ionic conductivities from DFT calculations and experimental confirmation, *Small*, 19, 2205122. <https://doi.org/10.1002/sml.202205122>.
- [23] Chakraborty, A.; Kunnikuruvan, S.; Kumar, S.; Markovsky, B.; Aurbach, D.; Dixit, M.; Major, D.T. (2020). Layered cathode materials for lithium-ion batteries: review of computational studies on $\text{LiNi}_{1-x-y}\text{Co}_x\text{Mn}_y\text{O}_2$ and $\text{LiNi}_{1-x-y}\text{Co}_x\text{Al}_y\text{O}_2$, *Chemistry of Materials*, 32, 915-952. <https://doi.org/10.1021/acs.chemmater.9b04066>.
- [24] Hua, W.; Schwarz, B.; Azmi, R.; Müller, M.; Darma, M.S.D.; Knapp, M.; Senyshyn, A.; Heere, M.; Missyul, A.; Simonelli, L. (2020). Lithium-ion (de) intercalation mechanism in core-shell layered $\text{Li}(\text{Ni},\text{Co},\text{Mn})\text{O}_2$ cathode materials, *Nano Energy*, 78, 105231. <https://doi.org/10.1016/j.nanoen.2020.105231>.
- [25] Chen, Y.; Yao, Y.; Yao, Z.; Li, W.; Shen, X.; Song, J.; Luan, W.; Chen, H.; Tu, S.-t.; Wu, K. (2025). Fracture behaviour of NCM polycrystalline particles in lithium-ion batteries under extreme conditions, *Nano Energy*, 141, 111104. <https://doi.org/10.1016/j.nanoen.2025.111104>.
- [26] Jiang, M.; Danilov, D.L.; Eichel, R.A.; Notten, P.H. (2021). A review of degradation mechanisms and recent achievements for Ni-rich cathode-based Li-ion batteries, *Advanced Energy Materials* 11, 2103005. <https://doi.org/10.1002/aenm.202103005>.
- [27] Lee, S.; Su, L.; Mesnier, A.; Cui, Z.; Manthiram, A. (2023). Cracking vs. surface reactivity in high-nickel cathodes for lithium-ion batteries, *Joule*, 7, 2430-2444. <https://doi.org/10.1016/j.joule.2023.09.006>.
- [28] Ryu, H.-H.; Park, K.-J.; Yoon, C.S.; Sun, Y.-K. (2018). Capacity fading of Ni-rich $\text{Li}[\text{Ni}_x\text{Co}_y\text{Mn}_{1-x-y}]\text{O}_2$ ($0.6 \leq x \leq 0.95$) cathodes for high-energy-density lithium-ion batteries: bulk or surface degradation? *Chemistry of Materials*, 30, 1155-1163. <https://doi.org/10.1021/acs.chemmater.7b05269>.
- [29] Primo, E.N., Chouchane, M.; Touzin, M.; Vazquez, P.; Franco, A.A. (2021). Understanding the calendaring processability of $\text{Li}(\text{Ni}_{0.33}\text{Mn}_{0.33}\text{Co}_{0.33})\text{O}_2$ -based cathodes, *Journal of Power Sources*, 488, 229361. <https://doi.org/10.1016/j.jpowsour.2020.229361>.
- [30] Alolaywi, H.; Uzun, K.; Cheng, Y.-T. (2025). Low porosity NMC622 and NMC811 electrodes made by severe calendaring, *Journal of Energy Storage*, 105, 114559. <https://doi.org/10.1016/j.est.2024.114559>.
- [31] Sim, R.; Lee, S.; Li, W.; Manthiram, A. (2021). Influence of calendaring on the electrochemical performance of $\text{LiNi}_{0.9}\text{Mn}_{0.05}\text{Al}_{0.05}\text{O}_2$ cathodes in lithium-ion cells, *ACS Applied Materials & Interfaces*, 13, 42898-42908. <https://doi.org/10.1021/acsami.1c12543>.
- [32] Lu, S.-j.; Tang, L.-b.; Wei, H.-x.; Huang, Y.-d.; Yan, C.; He, Z.-j.; Li, Y.-j.; Mao, J.; Dai, K.; Zheng, J.-c. (2022). Single-crystal nickel-based cathodes: fundamentals and recent advances, *Electrochemical Energy Reviews*, 5, 15. <https://doi.org/10.1007/s41918-022-00166-2>.
- [33] Shi, X.; Watanabe, T.; Yamamoto, K.; Kumar, M.; Thakur, N.; Matsunaga, T.; Fujii, M.; Kinoshita, H.; Iba, H.; Nagamine, M. (2024). Phase-transition-induced crack formation in $\text{LiNi}_{0.8}\text{Mn}_{0.1}\text{Co}_{0.1}\text{O}_2$

- cathode materials: a comparative study of single-crystalline and polycrystalline morphologies using Operando X-ray CT, *ACS Applied Energy Materials*, 7, 11144-11153. <https://doi.org/10.1021/acsaem.4c02340>.
- [34] Park, G.-T.; Ryu, H.-H.; Noh, T.-C.; Kang, G.-C.; Sun, Y.-K. (2022). Microstructure-optimized concentration-gradient NCM cathode for long-life Li-ion batteries, *Materials Today*, 52, 9-18. <https://doi.org/10.1016/j.mattod.2021.11.018>.
- [35] Rambukwella, I.; Ponnuru, H.; Yan, C. (2025). The role of dopants in mitigating the chemo-mechanical degradation of Ni-rich cathode: A critical review, *EcoEnergy*, 3, 321-353. <https://doi.org/10.1002/ece2.92>.
- [36] Belous, A.; Lisovskyi, I.; Khomenko, V. (2025). Surface modification of cathode materials with functional coatings for enhanced lithium-ion battery durability, *Journal of Applied Electrochemistry*, 55, 1963-1996. <https://doi.org/10.1007/s10800-025-02294-1>.
- [37] Wang, X.; Ruan, X.; Du, C.F.; Yu, H. (2022). Developments in surface/interface engineering of Ni-rich layered cathode materials, *The Chemical Record*, 22, e202200119. <https://doi.org/10.1002/tcr.202200119>.
- [38] Li, B.; Li, G.; Zhang, D.; Fan, J.; Chen, D.; Ge, Y.; Lin, F.; Zheng, C.; Li, L. (2019). Unveiling the impact of the polypyrrole coating layer thickness on the electrochemical performances of $\text{LiNi}_{0.5}\text{Co}_{0.2}\text{Mn}_{0.3}\text{O}_2$ in Li-ion battery, *ChemistrySelect*, 4, 6354-6360. <https://doi.org/10.1002/slct.201901112>.
- [39] Wang, L.; Su, Q.; Shi, W.; Wang, C.; Li, H.; Wang, Y.; Du, G.; Zhang, M.; Zhao, W.; Ding, S. (2022). Optimized structure stability and cycling performance of $\text{LiNi}_{0.8}\text{Co}_{0.1}\text{Mn}_{0.1}\text{O}_2$ through homogeneous nano-thickness Al_2O_3 coating, *Electrochimica Acta*, 435, 141411. <https://doi.org/10.1016/j.electacta.2022.141411>.
- [40] Maiti, S.; Curman, M.T.; Maiti, K.; Choung, S.; Han, J.W. (2023). Accelerating Li-based battery design by computationally engineering materials, *Chem*, 9, 3415-3460. <https://doi.org/10.1016/j.chempr.2023.09.007>.
- [41] Zhao, N.; Yi, S.; Wang, W.; Zhang, Y.; Luo, J.; Li, L.; Ning, T.; Tan, L.; Zou, K. (2025). Research and development of artificial intelligence in layered cathode materials for lithium-ion batteries, *Future Batteries*, 100093. <https://doi.org/10.1016/j.fub.2025.100093>.
- [42] Wang, L.; Lu, J. (2026). Marching towards cobalt-free cathode for lithium-ion battery, *Materials Today*, 95, 103284. <https://doi.org/10.1016/j.mattod.2026.103284>.



© 2026 by the authors. This article is an open access article distributed under the terms and conditions of the Creative Commons Attribution (CC BY) license (<http://creativecommons.org/licenses/by/4.0/>).